CFD study on the validity of using PCM in a controlled cooling ceiling integrated in a ventilated room

Youness Khattari, Ahmed Arid, Abdelmajid El Ouali, Tarik Kousksou, Isam Janajreh, El Mahjoub Ben Ghoulam

Version of Record: https://www.sciencedirect.com/science/article/pii/S2666165921000259
Manuscript_cffa87531398c161d18ea45e3f406258

CFD study on the validity of using PCM in a controlled cooling ceiling integrated in a ventilated room

Youness KHATTARI [a,*], Ahmed ARID [b], Tarik EL RHAFIKI [c], Tarik Kousksou [a], Isam Janajreh [d], El Mahjoub BEN GHOULAM [e]

[a] Université de Pau et des Pays de L'Adour, E2S UPPA, SIAME, Pau, France
[b] Ecole Nationale Supérieure d'Arts et Métiers (ENSAM), Moulay-Ismaïl University, Meknes, Morocco
[c] Engineering Sciences Laboratory, Polydisciplinary Faculty of Taza, Sidi Mohamed Ben Abdellah University Fez morocco
[d] Khalifa University of Science and Technology, Masdar campus, P.O. Box 54224, Abu Dhabi, United Arab Emirates
[e] Department of Physics, Faculty of Sciences, Moulay-Ismaïl University, Meknes, Morocco

Abstract

The aim of this work is to investigate the energy and thermal benefits of using PCM in a controlled cooling ceiling system integrated in a ventilated room, with three Moroccan climates representing three different Köppen-Geiger's climate types. The cooling power is controlled to maintain indoor air temperature in a narrow range assuring thermal comfort without wasting energy. Physical equations are solved numerically using computational fluid dynamics by a detailed 2D transient simulation integrating real ambient temperatures of Fez (Csa climate), Ifrane (Csb climate) and Marrakech (BSh climate). The main aim sought here is to assess the capacity of the paraffin C13 PCM to enhance the performance of a cooling ceiling system integrated in an efficiently ventilated room. Simulations performed justified the suitability of using the paraffin C13 PCM with the three climate types evaluated from a thermal point of view represented by the decreasing of fluctuation rate of the indoor air temperature, and with the Csa and

* Corresponding authors: Youness KHATTARI: khattariy@gmail.com

Csb climates represented by a saving of cooling power reaching 17.07 % and 16.30 %, respectively, from an energy-related point of view.

Keywords: CFD simulation; Phase change material; Cooling ceiling; Energy saving.

Highlights

- Numerical investigation on the validity of using PCM in a controlled cooling ceiling.
- Using the Paraffin C13 PCM in cooling ceiling led to a significant energy saving.
- Control of cooling power is applied to confine the indoor air temperature in a narrow interval contributing to the thermal comfort targeted.

Nomenclature

C_p specific heat ($Jkg^{-1}K^{-1}$)

f liquid fraction (%)

g gravity acceleration (ms^{-2})

h height of the opening for the air inlet or outlet (m)

H specific enthalpy (J/kg)

h_{ref} enthalpy at reference temperature (J/kg)

L latent heat of PCM (J/kg)

P fluid pressure (Pa)

$Q_{cooling}$ cooling power (W/m^2)

Re Reynolds number, Re $=(\rho_0 U_{in} h_{in})/ \mu_0$

T temperature (K)

t time (s)

u, w horizontal and vertical velocities (ms^{-1})

u^*, w^* dimensionless velocity components, $(u*, w*) = (u, w)/\sqrt{g\beta\Delta TL}$

U fluid velocity modulus (ms^{-1})

V fluid velocity vector (ms^{-1})

W specific humidity

X^*, Z^* dimensionless coordinates, $(X^*,Z^*) = (X,Z)/L$

Greek symbols

λ thermal conductivity ($Wm^{-1}K^{-1}$)

μ dynamic viscosity ($kgm^{-1}s^{-1}$)

ρ density (kgm^{-3})

Subscripts

in inlet

out outlet

1. Introduction

The world is actually facing several challenges concerning the energy sector, including climate change, the depletion of energy resources and rising costs for fossil energy that induced an interest to control global energy consumption generally and that related to buildings especially. The buildings sector accounts for around 40% of global energy consumption, and constitutes about 1/3 of world emissions of greenhouse gases [1,2]. Residential and commercial buildings accounts for approximately 60% of electricity consumption worldwide [3,4].

The energy challenges above-mentioned are widely amplified in Morocco as a country on the path to sustainable growth and development in this sector. Fossil fuels are the most used as energy sources, such as Petroleum that constitute over 61% of the overall energy consumption in Morocco [5]. The building sector is the most contributor of this national energy consumption in concordance with the increase of urbanization rate. As reported by the International Energy Agency (IEA), the Morocco's emissions of greenhouse gases were approximatively 42 $MtCO_2$ in 2008,

and based on the increase of energy consumption with 5.7% per year [6], Moroccan GHG emissions are estimated to be 153 MtCO2e in 2030 [2].

In order to control the excessive energy consumption in Morocco, the authorities have built the National Energy Strategy. It aims to improve the energy efficiency in all sectors by essentially expanding the use of renewable energies instead of fossil energies. As a main goal, 12% of energy saving must be achieved by 2020 and 15% by 2030 [7].

Space cooling is among the most energy consuming practices and greenhouse gas producers in building, especially when it concerns hot regions where cooling becomes a need for habitability and not just a commodity [8]. Therefore, many researches have been performed to study the capacity of some cooling systems to reduce the overall energy consumption while ensuring hygrothermal comfort and a good indoor air quality. In this case, radiant cooling systems can in some circumstances save up to 30% of energy consumption comparing with traditional convective cooling systems while maintaining a good level of thermal comfort [9–12]. Mosa et al. [13] Investigated the heat transfer and flow characteristics of a radiant cooling panel. They explored the role played by the flow architectures on the performance of the panel subjected to convection and radiation heat fluxes from the bottom in steady state by a numerical study. The authors presented also a comparison between serpentine and dendritic flow channels. Srivastava et al. [14] evaluated two new models in order to improve a Radiant Cooling System (RCS) efficiency. The RCS was coupled with a cooling tower in a first case and with a chiller in a second case. New systems were evaluated for different climatic conditions in India, and it was found that the cooling

tower-operated RCS recorded important annual energy savings compared to the chiller-operated RCS. Zhao and Liu [15] conducted a study on cooling systems in large space buildings and they found that radiant cooling systems present the most beneficial installation in terms of thermal comfort and energy saving. Seo et al. [16] suggested a new cooling system as a connection between radiant floor and forced convection cooling systems. They stated that this new hybrid system can save more that 20% of energy consumption compared to traditional cooling systems. Another study [17] claimed that if this forced convection system is a displacement ventilation system, this could not only prevent the condensation risk but also ameliorates the efficiency of ventilation and ensures better hygrothermal comfort. Zhang et al. [18] presented an advanced model simulating an underfloor ventilation coupled with radiant cooling ceiling, they compared the efficiency of two regulation components controlling the main system: a Model Predictive Control (MPC) and a conventional Proportional Integral Derivative (PID) controller. The results showed that the time to reach targeted hygrothermal comfort using PID controller was 13 minutes, and was 3 minutes using MPC controller under several experimental variations. These results justified the choice of the MPC controller as the main regulation system which reduced the energy consumption by 13.2% compared to PID controller. Earlier, the same author [19] proposed another dynamic resistance and capacity network model simulating the same system. Convective heat transfer coefficients, thermal capacities, and thermal resistances were determined by the least square method. Results justified the consistence of the model with a maximal relative error less than 8% between simulated and experimental values of ceiling heat flux. Lim et al. [20] searched for the

best configuration in terms of spacing and arrangement of thermoelectric modules in order to get uniform distribution of surface temperature. The authors developed a new model based on the finite difference method with a two-dimensional heat transfer analysis. The results showed that the most suitable configuration giving uniform distribution of surface temperature was the triangle one with 0.28 m spacing between the thermoelectric modules. Moosavi et al. [21] investigated the capacity of a hybrid evaporative cooling and solar chimney to provide an accepted thermal comfort in a naturally ventilated building under summer conditions. The efficiency of the cooling system was evaluated in terms of air movement and temperature of an atrium incorporated in the studied building. Results indicated that a larger air outlet in the solar chimney can increase the thermal comfort time by 30% with a reduction of cooling requirements reaching 12%. Su et al. [22] investigated the cooling capacity and heat transfer specifications of the concrete cooling ceiling. They were based on the finite difference method to develop a two dimensional model of heat transfer in order to obtain the surface temperature of the ceiling and the indoor air temperature, under different distances of tubes and supply water temperatures. Esparza L. et al. [23] tested the thermal performances of three roof evaporative cooling systems with three climate types: Hot sub-humid, warm sub-humid and hot humid. The first system was a water roof pond to serve as a reference, the second was a water roof pond with floating fabric and the third was a wet fabric as the innovative system corresponding to the no water consumption devices. Authors developed a mathematical model to simulate the performance of the new cooling system. Numerical results were compared against experimental measurements and they showed good agreement.

Using Phase Change Materials (PCM) with cooling systems is widely investigated in the literature recently due to their high energy storage capacity compared to conventional construction materials [24,25], many researches have been carried out to well understand end evaluate their features. Among them; Yasin et al. [26] Developed a new Trnsys model of a full scale room containing a cooling ceiling with PCM. The model was validated against experimental data of a real scale room. Results showed a good agreement between simulated and experimental data. Authors pretend to use the validated model for the optimization of the cooling ceiling control in a next work. Jobli et al. [27] assessed the thermal performances of a radiant cooling ceiling/wall integrating PCM, they coupled a hydronic capillary tube radiant panel with passive PCM for active building cooling and heating aim. The mathematical model is evaluated against a set of experiments and theoretical results showed good agreement with experimental values. Zhou et al. [28] proposed a hybrid renewable system integrating active PV cooling, hybrid ventilations and radiative cooling together with PCM' storages in order to improve the capacity of the cooling energy storage and to optimize the use of PV/T panels. In this work, an optimization approach was used for operating and geometrical parameters. The optimal parameters were presented in order to verify the validity of the optimization approach. Ansuini et al. [29] evaluated the energy saving capacity of a lightweight radiant cooling floor incorporating PCM in a room of 16 m². It was stated that the use of PCM in the cooling floor saved about 25% of the energy consumption related to cooling process. Moreover, the PCM was capable to maintain the comfort temperature between two and three days in between seasons as a result of their high thermal inertia.

Using radiant cooling systems must be taken with a special care, it could be accompanied with condensation if the temperature drops below dew point, which makes the indoor environment uncomfortable and unhealthy. Radiant cooling ceiling in office buildings of hot and humid climate was investigated by He et al. [30]. They remarked that in some circumstances of high level of humidity, the cooling ceiling was incapable to efficiently cool the indoor air. Lim et al. [31] claimed that the dew point is the most important parameter that should be taken into account when selecting the supply water temperature for floor cooling systems in buildings to prevent condensation. Novoselac and Srebric [32] presented some precautions to avoid condensation in residential buildings. They claimed that the exchange surface temperature of cooling system should be at least 1 °C higher than dew point. Moreover, an efficient ventilation system must be installed prior to the cooling component. Nutprasert and Chaiwiwatworakul [33] investigated a cooling system equipped with dehumidified air ventilation in tropical climate, they reported that comfortability of the indoor environment for this type of climates could not be assured without cooling and dehumidifying the fresh outside air.

To the authors' knowledge, research works reported in literature that have evaluated the performances of regulated cooling ceilings with and without macro-encapsulated PCM in ventilated rooms are limited. Thus, the main aim of the present work is to make a comparison between the performances of a regulated cooling ceiling with mortar-PCM versus another containing mortar only, which are both installed in an efficiently ventilated room [34,35] in order to compare their thermal efficiency and energy saving ability.

2. Numerical model

2.1. Physical model and methods

A sketch of the studied cavity is shown in Fig. 1. It is an efficiently ventilated square cavity [34,35] of dimensions 1.04 x 1.04 m² (adequate to compare results with experimental data of Blay et al. [36], and to fit in the range of scales practically acceptable by a CFD tool) filled with air and equipped by a regulated cooling ceiling. A PCM is integrated in the cooling ceiling in the first case as demonstrated in Fig. 1, and in a second case serving as a reference, the same physical model is duplicated excluding the PCM. The thermophysical properties of PCM capsules and mortar are indicated in Table 1. The distance between two PCM capsules is approximately 6.10^{-3} m. The distance between the bottom surface of the ceiling and the capsules is assumed to be around 5.10^{-3} m to easily recover the cooling energy stored inside the PCM.

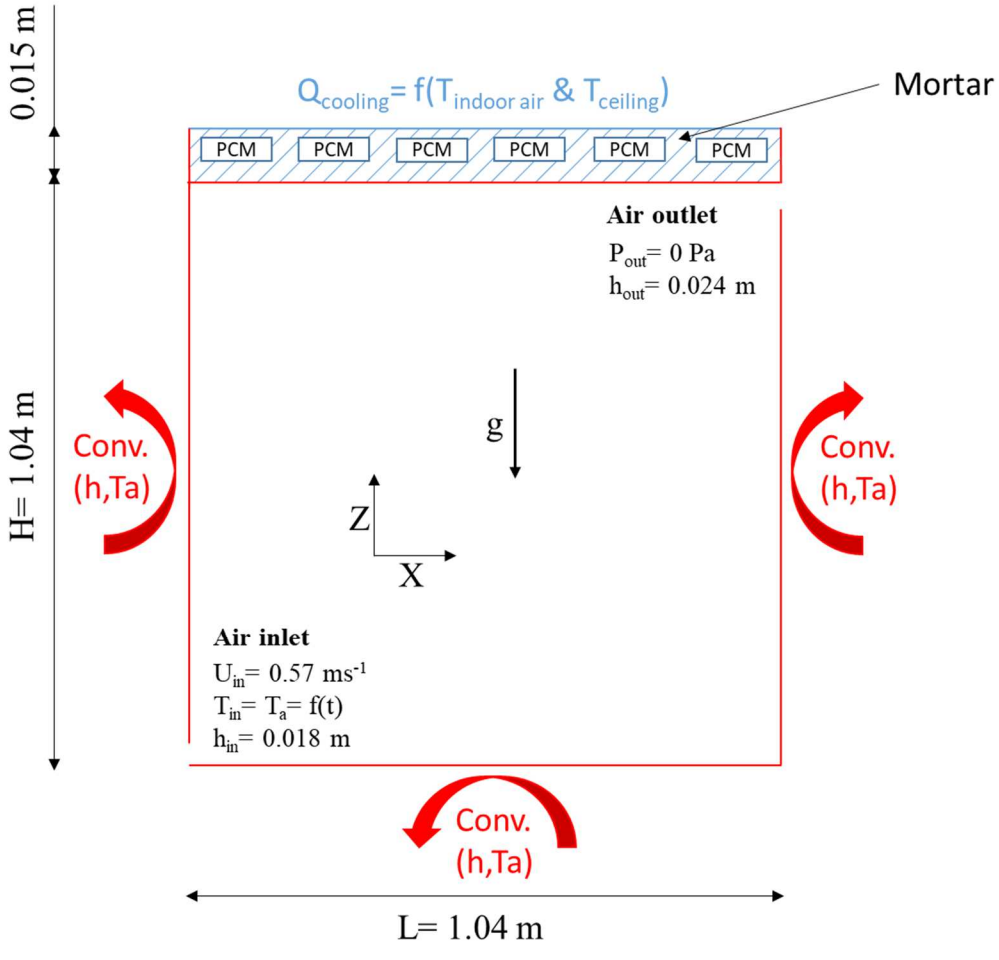

Fig. 1. Boundary conditions for the case of cooling ceiling with PCM

Table 1-a. Thermophysical properties of phase change material

Thermal conductivity	0.21 $W.m^{-1}.K^{-1}$
Density (solid)	0.9 $kg.m^{-3}$
Density (liquid)	0.76 $kg.m^{-3}$
Heat of fusion	189 $kJ.kg^{-1}$
Melting temperature (solidus – liquidus)	(22-24) °C

Table 1-b. Thermophysical properties of the mortar

Density	1400 $kg.m^{-3}$
Thermal conductivity	0.65 $W.m^{-1}.K^{-1}$
Specific heat capacity	925 $J.kg^{-1}.°C^{-1}$

In this work, a CFD tool was used to carry out the numerical simulations. A quadrilateral grid was applied to construct the computational domain using a meshing tool.

The hot air is introduced into the cavity via an inlet opening of 0.018 m with a fixed velocity of 0.57 $m.s^{-1}$ leading to a Reynolds number of Re=683, and extracted naturally through an outlet opening measuring 0.024 m. A User-Defined Function (UDF) was employed to use real and time-dependent ambient temperature (Ta) extracted from METEONORM software, of three Moroccan cities (Fez, Ifrane and Marrakech) as free stream temperature of convective walls and as inlet temperature of the 2D cavity shown in Fig. 1. In this study, the 24^{th} day of July with ten hours of simulation is considered (from 06h to 16h) to compare the performances of the cooling ceiling with PCM and without PCM in the three different Moroccan climates classified as Csa, Csb and BSh by the Köppen-Geiger climate classification for Fez, Ifrane and Marrakech, respectively (Fig. 2). The day 24th day of July was selected as it is considered to be among the hot days during the summer period.

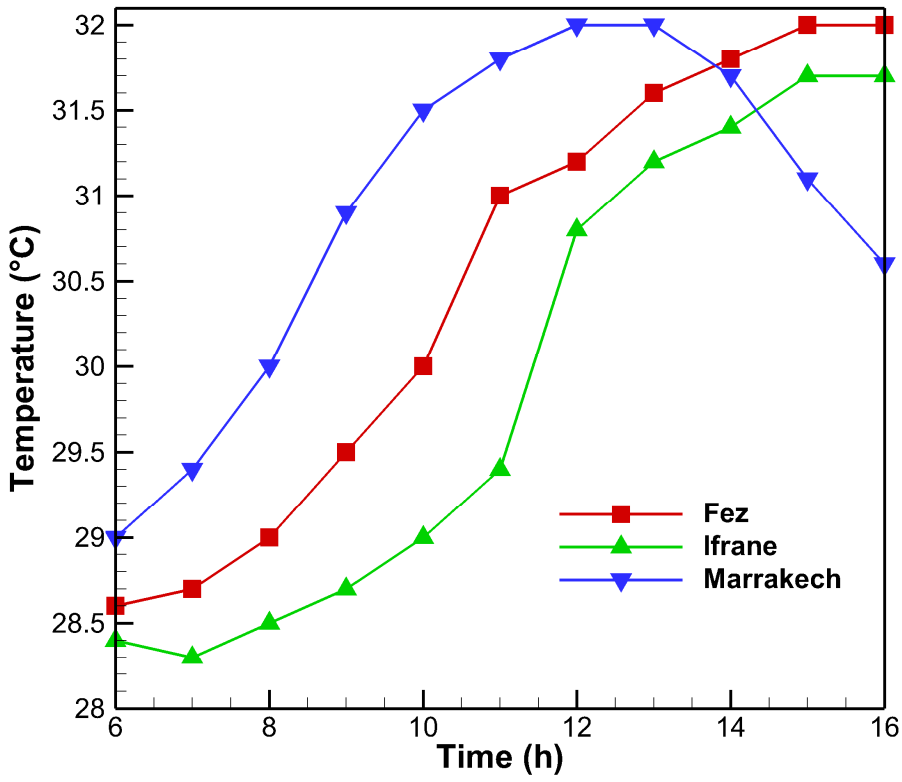

Fig. 2. Ambient temperatures of Fez, Ifrane and Marrakech on 24 July

In order to control the cooling ceiling power as a function of air mean temperature inside the cavity and the ceiling temperature, another UDF is used as follows: The UDF code reads the mean temperatures from the cavity ceiling and from the interior air, then, the cooling power will depend to these two values; if the mean temperature of the interior air is higher than 28 °C, the upper horizontal wall (blue wall in Fig. 1) is programmed as a heat flux wall with a value of -110 W/m² [37]. After, when the indoor air temperature drops below 26 °C, the cooling ceiling power turns off, and the upper horizontal wall is programmed as an adiabatic wall. These two latter operations are also executed if the ceiling temperature drops below 18 °C to avoid condensation risk [38]. A dead band of 2 K is programmed for this case to avoid fluctuation of the cooling power value.

The choice of PCM for cooling ceiling systems must be done with particular care. Selected PCM must have such features as right temperature in phase transition, chemical stability, sufficient latent heat and acceptable price. Based on these criteria, the PCM used here is the paraffin C13 [39] which has proved to be one of the most promising PCM in the case of cooling ceiling systems. The dimensions of one PCM block are selected to be 0.01 x 0.006 m² with a total number of 21 equidistant blocks.

2.2. Mathematical formulation

2.2.1. Airflow inside the square cavity

To investigate the airflow through the cavity and the heat transfer through the ceiling, a number of assumptions have been made:

- The air is Newtonian and incompressible.

- Both viscous dissipation and heat transfer by radiation are negligible.
- Airflow inside the cavity is turbulent and unsteady.
- Thermophysical properties of air are supposed to be constant, excluding the buoyancy force terms, which are simulated by the Boussinesq approximation.
- Only the heat transfer by conduction was considered in the ceiling.
- Due to the small size of the PCM capsules, natural convection during the phase change process is neglected.

Using the above hypotheses, the average equations describing airflow inside the square cavity are as follows:

$$\frac{\partial \rho_a}{\partial t}+\frac{\partial}{\partial x_j}\left(\rho_a U_{j,a}\right)=0 \quad \textbf{(1)}$$

$$\frac{\partial\left(\rho_a U_{i,a}\right)}{\partial t}+\frac{\partial}{\partial x_j}\left(\rho_a U_{i,a}U_{j,a}\right)=-\frac{\partial p}{\partial x_i}+\frac{\partial}{\partial x_j}\left[\mu\left(\frac{\partial U_{i,a}}{\partial x_j}+\frac{\partial U_{j,a}}{\partial x_i}\right)\right]+\frac{\partial}{\partial x_j}\left(-\rho_a\overline{u_{i,a}u_{j,a}}\right) \quad \textbf{(2)}$$
$$+\rho_a g_i\beta\left(T_a-T_o\right)$$

$$\frac{\partial\left(\rho_a T_a\right)}{\partial t}+\frac{\partial}{\partial x_j}\left(\rho_a T_a U_{j,a}\right)=\frac{\partial}{\partial x_j}\left(\frac{\mu}{\mathrm{Pr}}\frac{\partial T_a}{\partial x_j}\right)+\frac{\partial}{\partial x_j}\left(-\rho_a\overline{u_{j,a}T_a^{'}}\right) \quad \textbf{(3)}$$

where $-\rho_a\overline{u_{i,a}u_{j,a}}$ and $-\rho_a\overline{u_{j,a}T_a^{'}}$ represent the Reynolds stresses and the turbulent heat flux, respectively which can be determined using the following equations:

$$\rho_a\overline{u_{i,a}u_{j,a}}=\frac{2}{3}\rho_a k\delta_{ij}+\frac{2}{3}\mu_{t,a}\delta_{ij}\frac{\partial U_{j,a}}{\partial x_j}-\mu_{t,a}.\left(\frac{\partial U_{i,a}}{\partial x_j}+\frac{\partial U_{j,a}}{\partial x_i}\right) \quad \textbf{(4)}$$

$$\rho_a\overline{u_{j,a}T_a^{'}}=-\frac{\mu_{t,a}}{\mathrm{Pr}_{t,a}}\frac{\partial T_a}{\partial x_j} \quad \textbf{(5)}$$

where $k = \frac{\overline{u_{i,a} u_{j,a}}}{2}$ is the turbulent kinetic energy, $\mu_{t,a}$ is the eddy viscosity, and $\mathrm{Pr}_{t,a}$ is the turbulent Prandtl number.

The system of equations **(1-5)** needs to be closed by considering the transport equations for turbulent kinetic energy (k) and its dissipation rate (ε).

$$\frac{\partial(\rho_a k)}{\partial t} + \frac{\partial}{\partial x_j}(\rho_a k U_{j,a}) = \frac{\partial}{\partial x_j}\left[\sigma_k(\mu + \mu_t)\frac{\partial k}{\partial x_j}\right] + G_s + G_t - \rho_a.\varepsilon \quad \textbf{(6)}$$

$$\frac{\partial(\rho_a \varepsilon)}{\partial t} + \frac{\partial}{\partial x_j}(\rho_a \varepsilon U_{j,a}) = \frac{\partial}{\partial x_j}\left[\sigma_\varepsilon(\mu + \mu_t)\frac{\partial \varepsilon}{\partial x_j}\right] + G_1(G_S + G_t)(1 + C_3 R_f)\left(\frac{\varepsilon}{k}\right) - C_2\left(\frac{\rho_a \varepsilon^2}{k}\right) \quad \textbf{(7)}$$

where G_S is the producing shear rate of turbulent kinetic energy, G_t is the buoyancy generation rate of turbulent kinetic energy and σ_k, σ_e, C_1, C_2, C_3 and C_μ are the physical constant of the numerical model [34].

The convection heat transfer mode is applied to the vertical walls and the floor with a free stream temperature of Ta and a heat transfer coefficient h imposed by the Moroccan Agency for Energy Efficiency (AMEE) as a function of the climatic zone [40] (see table 2).

Table 2. Building thermal requirements imposed by the AMEE for the six Moroccan climatic zones

Climatic zone	$U_{Ceiling}$ (W/m²K)	U_{Walls} (W/m²K)	R_{Floor} (m²K/W)
Zone 1 – Agadir	0.75	1.20	No requirement
Zone 2 – Tangier	0.75	0.80	No requirement
Zone 3 – Fez	0.65	0.80	0.75
Zone 4 – Ifrane	0.55	0.60	1.25

Zone 5 – Marrakech	0.65	0.80	1.00
Zone 6 – Errachidia	0.65	0.80	1.00

2.2.2. Heat diffusion across the ceiling

As the ceiling consists of two materials (mortar and PCM), the diffusion of heat across it can be studied using the following equation:

$$\rho_{mr,pcm}\frac{\partial H_{mr,pcm}}{\partial t}=\nabla.\left(\lambda_{mr,pcm}\nabla T_{mr,pcm}\right) \quad \textbf{(8)}$$

where $\rho_{mr,pcm}$ (density), $\lambda_{mr,pcm}$ (thermal conductivity) and $H_{mr,pcm}$ (specific enthalpy) are the thermophysical properties of mortar or PCM.

For PCM, the specific enthalpy can be calculated using the following expression:

$$H_{PCM}=H_{ref}+\int_{T_{ref}}^{T}C_{PCM}dT+\phi.L_f \quad \textbf{(9)}$$

The liquid fraction ϕ in Eq.9 has been evaluated at each control volume inside the ceiling using the following expressions:

$$\begin{cases}\phi=0 \quad if\ T_{PCM}<T_{PCM,S}\\ \phi=\dfrac{T_{PCM}-T_{PCM,S}}{T_{PCM,L}-T_{PCM,S}} \quad if\ T_{PCM,S}<T_{PCM}<T_{PCM,L}\\ \phi=1 \quad if\ T_{PCM}>T_{PCM,L}\end{cases} \quad \textbf{(10)}$$

Where L_m is the latent heat of melting/solidification. $T_{PCM,L}$ is the liquidus temperature and $T_{PCM,S}$ is the solidus temperature of the PCM.

2.3. Validation and verification

Results extracted from every numerical code must be verified and validated against available data in literature. Therefore, our numerical code was validated in the cases of

the two physical phenomena cited above (section 2.2). Firstly, the code was validated in the case of heat transfer by mixed convection in a ventilated cavity heated from below in turbulent and steady flow (Fig. 3). Secondly, the code was validated in the case of heat transfer within a PCM wallboard (Fig. 4).

The first problem was investigated by Blay et al. [36]. A ventilated cavity filled with air and heated from below was the field study of this work. A temperature of 35.5 °C was selected for the bottom wall. The other walls are maintained at a temperature of 15 °C. The air is introduced to the cavity with a velocity of 0.57 ms^{-1} and a temperature of 15 °C at the top of the left vertical wall, and extracted naturally from the bottom of the right vertical wall. Comparisons performed are presented in Fig. 3 in terms of temperature (T) and velocity components (u and w) at the middle of the cavity (X*=0.5 or Z*=0.5). Results showed that there is an insignificant difference between our predictions and experimental data. The velocities profiles and temperature are almost identical.

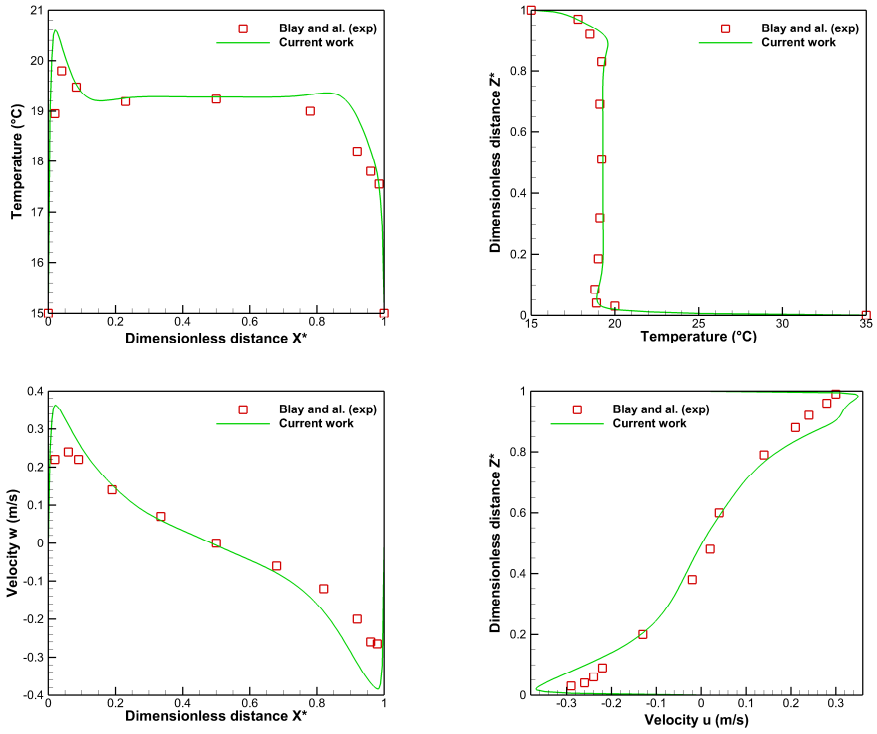

Fig. 3. Comparison of temperature and velocity with experimental data of Blay et al. [37]

The second problem was studied by Zhou et al. [41]. It consists of analyzing the heat transfer within a shape-stabilized PCM (SSPCM) wallboard (see Fig.4). It is assumed that the PCM is dispersed uniformly in the building material. The outside surface of the wallboard is assumed to be under sinusoidal heat flux (see Eq.11). The inside face of the wallboard, convection boundary condition is used and the average air temperature inside the room is maintained constant at 20°C (see Eq.12). The PCM investigated in the context of this problem is supposed pure.

$$q_{out} = -k_c \left.\frac{\partial T}{\partial x}\right|_{x=0} \tag{11}$$

$$K_{in}\big(20 - T(x = L, t)\big) = -k_c \left.\frac{\partial T}{\partial x}\right|_{x=L} \tag{12}$$

Where K_{in} is the inner convective heat transfer coefficient.

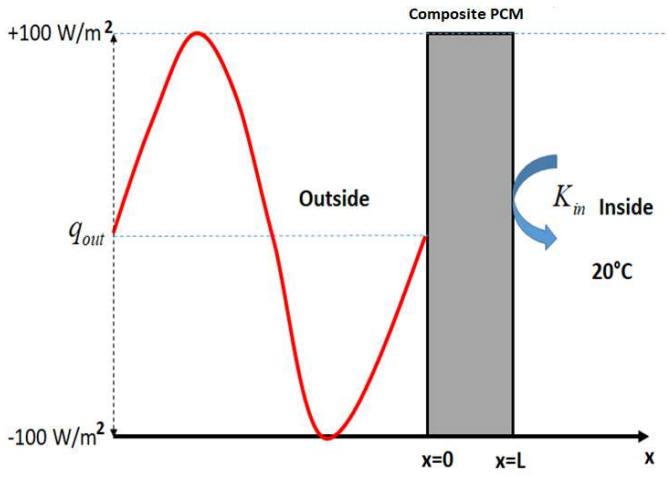

Fig. 4. SSPCM wallboard under sinusoidal heat flux

The thermophysical properties of the SSPCM wallboard used by Zhou et al. [41] are shown in Table 3.

Table 3. Thermophysical properties and convective heat transfer coefficient for the SSPCM wallboard

ρ (kg.m^{-3})	850
k (W.m^{-1}.K^{-1})	0.2
c_S (J.kg^{-1}°C^{-1})	2000
c_L (J.kg^{-1}°C^{-1})	2000
L_f (J.g^{-1})	120
T_m(°C)	292-294
K_{in}(W.m^{-2}.K^{-1})	8.7
L(m)	0.02

Fig.5 displays a comparison between the hourly inner heat flux obtained by our physical model and that obtained by Zhou et al. [41]. A total number of 1960 cells was found to be acceptable in this case. As shown in Fig.5, there is a good agreement between our results and those obtained by Zhou et al. [41]. One can observe the good capability of our model to predict the melting (charging) and crystallization (discharging) processes inside SSPCM wallboard.

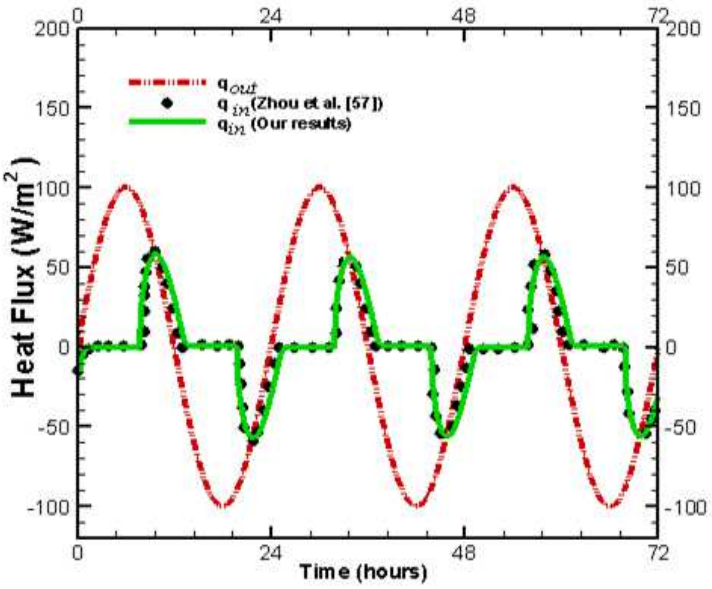

Fig. 5.Inner heat flux versus time

From the above comparisons, it can be seen that our numerical code developed for the case of this work provides satisfactory results.

3. Results and discussion

To deepen our knowledge on the validity of using PCM and study their benefits during the summer period, several numerical simulations are performed analyzing the performance of a cooling ceiling composed of PCM and mortar in a first case, and another composed of mortar only in a second case. The cooling ceiling power is controlled in such a way as to obtain an indoor air temperature fluctuating between 26 °C (known as the comfort temperature) and 28 °C (known as the economic comfort temperature) regardless of the external temperature, while keeping the ceiling temperature above a critical value of 18 °C to avoid condensation. Real fluctuating ambient temperature for three different Moroccan cities were included in the simulation process.

Before proceeding to the simulations, results independence with respect to the mesh and the time step was assured. We have recorded at a specific time the average value of the air temperature inside the square cavity, the ceiling temperature and the liquid fraction of the PCM (see table 4). From Table 4, we can confirm that the fine mesh and the time step of 0.1 second provide satisfactory results.

Table 4-a. Results of the grid independence test

	Coarse mesh (25102 cells)	Medium mesh (46265 cells)	Fine mesh (65624 cells)	Very fine mesh (84916 cells)
Indoor air temperature [°C]	26.13	26.20	26.25	26.29
Ceiling temperature [°C]	21.11	21.83	22.54	22.67
Liquid fraction in PCM	0.161	0.169	0.176	0.179

Table 4-b. Results of the time step independence test

Time step	10 seconds	1 second	0.1 seconds	0.01 seconds
Indoor air temperature [°C]	26.34	26.30	26.25	26.24
Ceiling temperature [°C]	23.51	23.06	22.54	22.46
Liquid fraction in PCM	0.183	0.18	0.176	0.174

3.1. Performance of the cooling ceiling incorporating PCM

A plot of the indoor air temperature of the ventilated room, ceiling temperature, liquid fraction in PCM blocks and cooling power in the case of the cooling ceiling integrating PCM for the cities of Fez, Ifrane and Marrakech is presented in Fig. 6. It

can be noted that the four graphs are widely different from a city to another, this can be justified by the fact that the three Moroccan cities have different types of climate according to the Köppen-Geiger climate classification.

The simulation process can be described as follows: the overall initial temperature is set at 28 °C, as it is greater than or equal to the set-point temperature of 28 °C, the cooling power is set to 110 W/m². Thus, the ceiling temperature and the indoor air temperature begin to decrease with different intensities based on the type of external climate. After, when the minimum temperature of 26 °C is reached for the indoor air of the room, or if the ceiling temperature drops below the critical value of 18 °C, the cooling power turns to 0 W/m². As a result, the ceiling temperature and the indoor air temperature increase with respect to time until the latter reaches 28 °C again due to the hot external climate. This process is repeated while the ten hours of simulation are not completed. The number of cycles of cooling/heating in Fez was five, in Ifrane was four and in Marrakech was five and a half cycles. This confirmed that the Marrakech's climate is the warmer between the three chosen Moroccan climates. It can be seen also that the indoor air temperature and the ceiling temperature may slightly drop below their minimum temperatures, this is a direct result of the inertia of interior air and the mortar integrating PCM when the cooling power is turned off.

Regarding the ceiling temperature in Fez for example, its maximum reached 25.4 °C by the end of the first cycle of cooling/heating. By the end of the second cycle, the maximum of the same temperature has decreased by 1.4 °C and reached almost 24 °C. This decreases in the maximal temperatures of the ceiling have continued until the end of simulation. This can be explained by the fact that the external temperature of the

period simulated was an increasing function with respect to time. Thus, while cycles are passing, the maximum of the indoor air temperature is reached faster and the cooling is started again before the ceiling maximal temperature of the previous cycle is reached. Identical reasoning can be adapted to justify the increases of indoor air temperature in several cycles before reaching its minimal value of 26 °C in Marrakech for instance.

Concerning the liquid fraction in the PCM blocks, it can be seen from Fig. 5 that it is in good concordance with the other thermal parameters of the simulation. At the start of the simulation, the liquid fraction value is one, which means that all PCM blocks are in their liquid form. The liquid fraction value of one remains constant within a specified time period even if the cooling power is turned on, this is because the initial temperature of the PCM blocks is 28 °C, and they continue to lose sensible energy and to drop their temperature until this latter reaches the melting temperature. Then, under the cooling power, the PCM begins the solidification process and the liquid fraction drops down. When the cooling power turns off, the liquid fraction starts to rise up with the melting process of PCM blocks due to the hot external climate, delaying then the warming of the mortar and interior air domains.

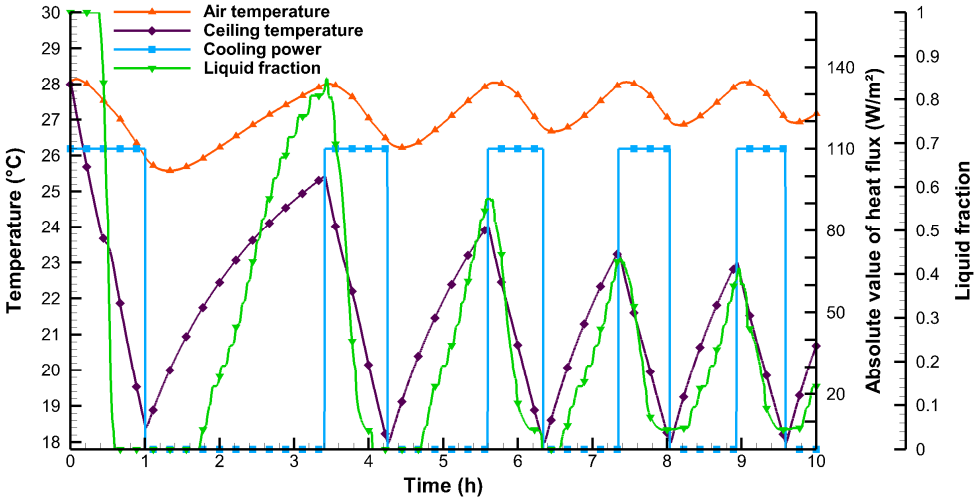

(a)

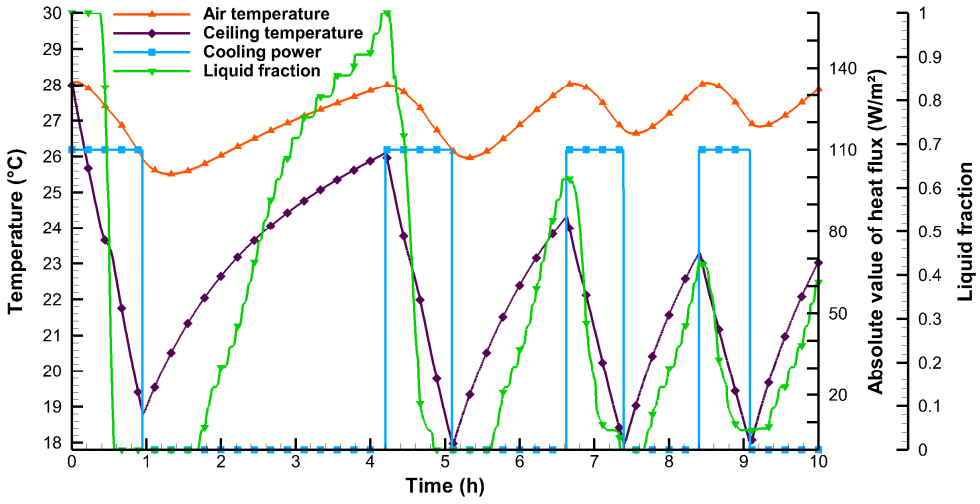

(b)

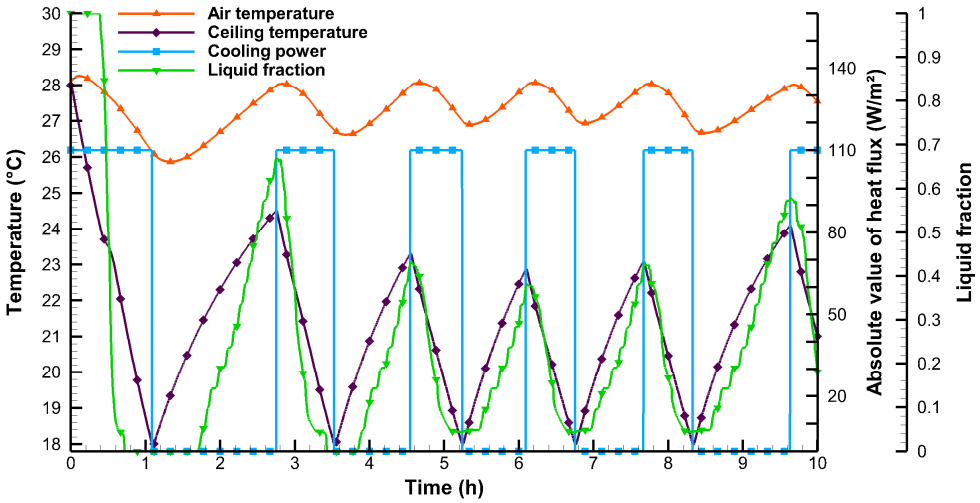

(c)

Fig. 4. Thermal characteristics of the room with cooling ceiling containing PCM for Fez (a), Ifrane (b) and Marrakech (c)

3.2. Performances of the cooling ceiling without PCM

A plot of the cooling power, floor temperature and indoor air temperature of the ventilated room in the case of the cooling ceiling without PCM for the three Moroccan cities studied is presented in Fig. 7. As can be noted, even without PCM, the minimal temperatures of the indoor air and the ceiling are slightly exceeded as a result of the same above-mentioned reason (section 3.1).

All what is said about the decreasing of the maximal ceiling temperature, and the increasing of the minimal indoor air temperature with respect to the number of cycles in the previous section remain valid in this case also. In Ifrane for example, the minimal indoor air temperature increased by 0.6 °C from the third cycle to the fourth, and by 0.3 °C from the fourth cycle to the fifth. Concerning the maximal ceiling temperature in the same city, it decreased by 1.3 °C from the first cycle to the second, and by 1.6 °C from the second cycle to the third.

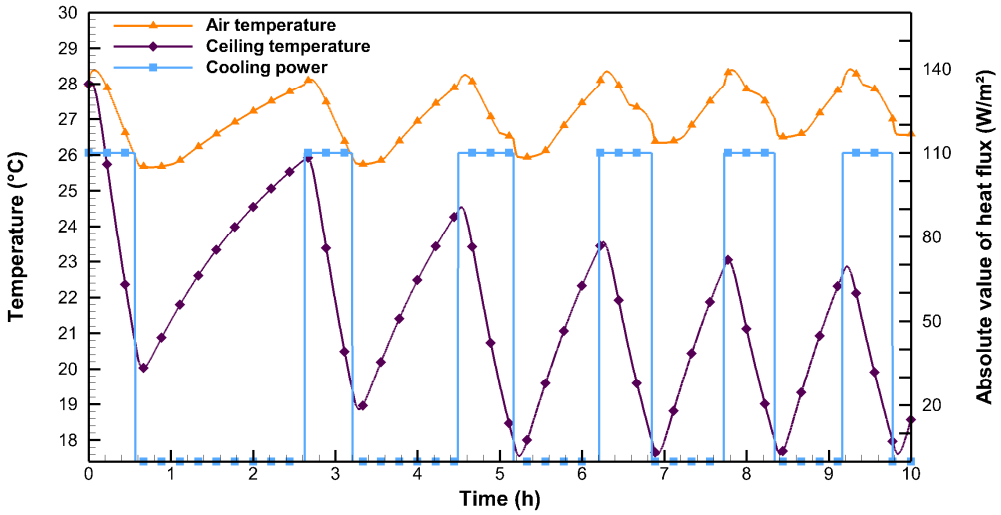

(a)

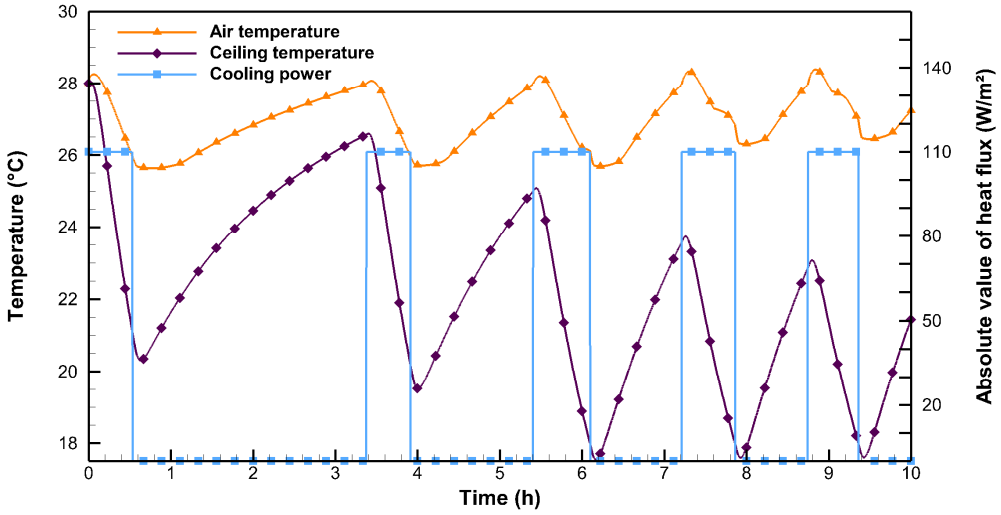

(b)

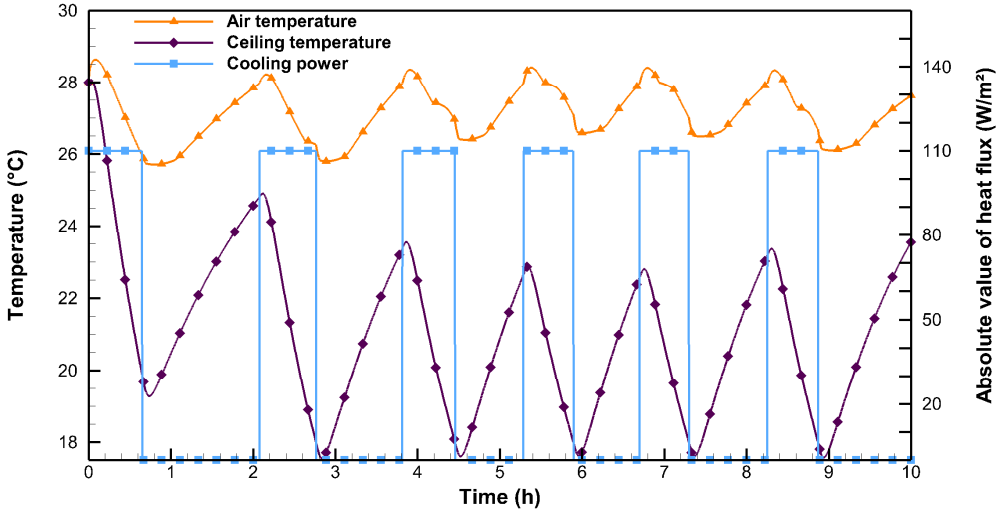

(c)

Fig. 5. Thermal characteristics of the room containing cooling ceiling without PCM for Fez (a), Ifrane (b) and Marrakech (c)

3.3. Validity of using PCM with the controlled cooling ceiling

It is useful to recall that the main aim behind this study is to compare the performances of a controlled cooling ceiling integrating PCM with another without PCM in a ventilated room. By comparing the two cases, one can observe that when the electrical cooling power is turned off, the average air temperature inside the cavity without PCM increases quite rapidly compared to that in the cavity with PCM. This can be explained by the thermal inertia of the PCM during the phase change process. During the cooling process via electrical source, the PCM works as thermal energy storage, it stores cooling energy during the time when the cooling power is turned on. Once the cooling energy is stored in the PCM, we turn off the electrical source. Switching off the electrical source leads to an increase in temperature at ceiling level, which causes melting of the PCM. The melting is generally carried out at a constant temperature and at the same time it is accompanied by an absorption of heat from the cavity at ceiling level. During the melting process, the ceiling temperature is kept close to the PCM melting temperature. To evaluate the benefits of the cooling ceiling system, we calculated the electrical energy consumed by the electrical source (see Eq.13) installed in the ceiling with and without PCM.

$$\text{Energy saving} = \frac{\text{Energy consumption without PCM - Energy consumption with PCM}}{\text{Energy consumption without PCM}} \quad (13)$$

Results of energy consumptions and energy savings by using PCM in the three cities are reported in Table 5.

Table 5. Energy savings by using PCM in cooling ceiling for Fez, Ifrane and Marrakech

Cities	Köppen-Geiger's climate types	Energy consumptions [kJ]		Energy savings [%]
		With PCM	Without PCM	
Fez	Csa	1208.12	1456.76	+17.07
Ifrane	Csb	1086.31	1297.90	+16.30
Marrakech	BSh	1472.23	1505.89	+02.23

As shown in table 5, using the paraffin C13 as PCM in cooling ceiling for the Csa and Csb Köppen-Geiger's climate types yielded to an energy savings of 17.07 % and 16.30 %, respectively. For the BSh type, the cooling energy consumption decreased by just 02.23 % by using the above-mentioned PCM. Thus, it can be concluded that the paraffin C13 is not beneficial enough for this type of Köppen-Geiger's climates, and more researches must be conducted to find an appropriate PCM for this case.

4. Conclusion

The validity of using PCM in a regulated cooling ceiling integrated in an efficiently ventilated room was computationally assessed. The cooling ceiling was incorporating the paraffin C13 PCM in a case, and contained mortar only in a second case serving as a reference. The main aim was to investigate the thermal and energy-related performances of the regulated cooling ceiling with three different Moroccan Köppen-Geiger climates. Simulations have been carried out under a turbulent and transient flow regime integrating real fluctuating ambient temperature by using a UDF. This latter is also used for controlling the cooling power as a function of the ceiling and the indoor air temperatures. Results showed that the use of paraffin C13 as PCM in

cooling ceiling with the climates of Fez and Ifrane was beneficial with an energy savings of 17.07 % and 16.30 %, respectively. It has been found also that energy consumption decreased by just 02.23 % with Marrakech's climate by using the paraffin C13, as a result, it is considered as not sufficiently beneficial for this type of climates.

Acknowledgements

The financial support received from the Moroccan National Centre for Scientific and Technical Research (CNRST) is highly acknowledged.

References

[1] B. Nourozi, Q. Wang, A. Ploskić, Energy and defrosting contributions of preheating cold supply air in buildings with balanced ventilation, Appl. Therm. Eng. 146 (2019) 180–189. https://doi.org/10.1016/j.applthermaleng.2018.09.118.

[2] A. Allouhi, Y. El Fouih, T. Kousksou, A. Jamil, Y. Zeraouli, Y. Mourad, Energy consumption and efficiency in buildings: current status and future trends, J. Clean. Prod. 109 (2015) 118–130. https://doi.org/10.1016/j.jclepro.2015.05.139.

[3] T. Kousksou, A. Allouhi, M. Belattar, A. Jamil, T. El Rhafiki, A. Arid, Y. Zeraouli, Renewable energy potential and national policy directions for sustainable development in Morocco, Renew. Sustain. Energy Rev. 47 (2015) 46–57. https://doi.org/10.1016/j.rser.2015.02.056.

[4] S. ed-Dîn Fertahi, T. Bouhal, F. Gargab, A. Jamil, T. Kousksou, A. Benbassou, Design and thermal performance optimization of a forced collective solar hot water production system in Morocco for energy saving in residential buildings, Sol. Energy. 160 (2018) 260–274. https://doi.org/10.1016/j.solener.2017.12.015.

[5] Ministère de l'Energie, des Mines, de l'Eau et de l'Environnement (MEMEE), Les Energies Renouvelables au Maroc: Stratégie et plan d'action, Casablanca. (2012).

[6] N. Supersberger, L. Führer, Integration of renewable energies and nuclear power into North African Energy Systems: An analysis of energy import and export effects, Energy Policy. 39 (2011) 4458–4465. https://doi.org/10.1016/j.enpol.2010.12.046.

[7] T. Kousksou, A. Allouhi, M. Belattar, A. Jamil, T. El Rhafiki, Y. Zeraouli, Morocco's strategy for energy security and low-carbon growth, Energy. 84 (2015) 98–105. https://doi.org/10.1016/j.energy.2015.02.048.

[8] J.A. Castillo, R. Tovar, Transient cooling of a room with a chilled ceiling, Sol. Energy. 86 (2012) 1029–1036. https://doi.org/10.1016/j.solener.2011.06.026.

[9] J. Miriel, L. Serres, A. Trombe, Radiant ceiling panel heating–cooling systems: experimental and simulated study of the performances, thermal comfort and energy consumptions, Appl. Therm. Eng. 22 (2002) 1861–1873. https://doi.org/10.1016/S1359-4311(02)00087-X.

[10] T. Kim, S. Kato, S. Murakami, J. Rho, Study on indoor thermal environment of office space controlled by cooling panel system using field measurement and the numerical simulation, Build. Environ. 40 (2005) 301–310. https://doi.org/10.1016/j.buildenv.2004.04.010.

[11] H.E. Feustel, C. Stetiu, Hydronic radiant cooling — preliminary assessment, Energy Build. 22 (1995) 193–205. https://doi.org/10.1016/0378-7788(95)00922-K.
[12] R.A. Memon, S. Chirarattananon, P. Vangtook, Thermal comfort assessment and application of radiant cooling: A case study, Build. Environ. 43 (2008) 1185–1196. https://doi.org/10.1016/j.buildenv.2006.04.025.
[13] M. Mosa, M. Labat, S. Lorente, Role of flow architectures on the design of radiant cooling panels, a constructal approach, Appl. Therm. Eng. (2018). https://doi.org/10.1016/j.applthermaleng.2018.12.107.
[14] P. Srivastava, Y. Khan, M. Bhandari, J. Mathur, R. Pratap, Calibrated simulation analysis for integration of evaporative cooling and radiant cooling system for different Indian climatic zones, J. Build. Eng. 19 (2018) 561–572. https://doi.org/10.1016/j.jobe.2018.05.024.
[15] F.-Y. Zhao, D. Liu, G.-F. Tang, Application issues of the streamline, heatline and massline for conjugate heat and mass transfer, Int. J. Heat Mass Transf. 50 (2007) 320–334. https://doi.org/10.1016/j.ijheatmasstransfer.2006.06.026.
[16] J.-M. Seo, D. Song, K.H. Lee, Possibility of coupling outdoor air cooling and radiant floor cooling under hot and humid climate conditions, Energy Build. 81 (2014) 219–226. https://doi.org/10.1016/j.enbuild.2014.06.023.
[17] F. Causone, F. Baldin, B.W. Olesen, S.P. Corgnati, Floor heating and cooling combined with displacement ventilation: Possibilities and limitations, Energy Build. 42 (2010) 2338–2352. https://doi.org/10.1016/j.enbuild.2010.08.001.
[18] D. Zhang, X. Huang, D. Gao, X. Cui, N. Cai, Experimental study on control performance comparison between model predictive control and proportion-integral-derivative control for radiant ceiling cooling integrated with underfloor ventilation system, Appl. Therm. Eng. 143 (2018) 130–136. https://doi.org/10.1016/j.applthermaleng.2018.07.046.
[19] D. Zhang, X. Xia, N. Cai, A dynamic simplified model of radiant ceiling cooling integrated with underfloor ventilation system, Appl. Therm. Eng. 106 (2016) 415–422. https://doi.org/10.1016/j.applthermaleng.2016.06.017.
[20] H. Lim, Y.-K. Kang, J.-W. Jeong, Thermoelectric radiant cooling panel design: Numerical simulation and experimental validation, Appl. Therm. Eng. 144 (2018) 248–261. https://doi.org/10.1016/j.applthermaleng.2018.08.065.
[21] L. Moosavi, M. Zandi, M. Bidi, Experimental study on the cooling performance of solar-assisted natural ventilation in a large building in a warm and humid climate, J. Build. Eng. 19 (2018) 228–241. https://doi.org/10.1016/j.jobe.2018.04.026.
[22] L. Su, N. Li, X. Zhang, Y. Sun, J. Qian, Heat transfer and cooling characteristics of concrete ceiling radiant cooling panel, Appl. Therm. Eng. 84 (2015) 170–179. https://doi.org/10.1016/j.applthermaleng.2015.03.045.
[23] C.J. Esparza L., C. Escobar del Pozo, A. Gómez A., G. Gómez A., E. Gonzalez C., Potential of a wet fabric device as a roof evaporative cooling solution: Mathematical and experimental analysis, J. Build. Eng. 19 (2018) 366–375. https://doi.org/10.1016/j.jobe.2018.05.021.
[24] C. Fabiani, C. Piselli, A.L. Pisello, Thermo-optic durability of cool roof membranes: Effect of shape stabilized phase change material inclusion on building energy efficiency, Energy Build. 207 (2020) 109592. https://doi.org/10.1016/j.enbuild.2019.109592.
[25] Y.K. Yang, M.Y. Kim, M.H. Chung, J.C. Park, PCM cool roof systems for mitigating urban heat island - an experimental and numerical analysis, Energy Build. 205 (2019) 109537. https://doi.org/10.1016/j.enbuild.2019.109537.
[26] M. Yasin, E. Scheidemantel, F. Klinker, H. Weinläder, S. Weismann, Generation of a simulation model for chilled PCM ceilings in TRNSYS and validation with real scale building data, J. Build. Eng. 22 (2019) 372–382. https://doi.org/10.1016/j.jobe.2019.01.004.

[27] M.I. Jobli, R. Yao, Z. Luo, M. Shahrestani, N. Li, H. Liu, Numerical and experimental studies of a Capillary-Tube embedded PCM component for improving indoor thermal environment, Appl. Therm. Eng. 148 (2019) 466–477. https://doi.org/10.1016/j.applthermaleng.2018.10.041.
[28] Y. Zhou, S. Zheng, G. Zhang, Multivariable optimisation of a new PCMs integrated hybrid renewable system with active cooling and hybrid ventilations, J. Build. Eng. 26 (2019) 100845. https://doi.org/10.1016/j.jobe.2019.100845.
[29] R. Ansuini, R. Larghetti, A. Giretti, M. Lemma, Radiant floors integrated with PCM for indoor temperature control, Energy Build. 43 (2011) 3019–3026. https://doi.org/10.1016/j.enbuild.2011.07.018.
[30] Y. He, N. Li, Q. Huang, A field study on thermal environment and occupant local thermal sensation in offices with cooling ceiling in Zhuhai, China, Energy Build. 102 (2015) 277–283. https://doi.org/10.1016/j.enbuild.2015.05.058.
[31] J.-H. Lim, J.-H. Jo, Y.-Y. Kim, M.-S. Yeo, K.-W. Kim, Application of the control methods for radiant floor cooling system in residential buildings, Build. Environ. 41 (2006) 60–73. https://doi.org/10.1016/j.buildenv.2005.01.019.
[32] A. Novoselac, J. Srebric, A critical review on the performance and design of combined cooled ceiling and displacement ventilation systems, Energy Build. 34 (2002) 497–509. https://doi.org/10.1016/S0378-7788(01)00134-7.
[33] N. Nutprasert, P. Chaiwiwatworakul, Radiant Cooling with Dehumidified Air Ventilation for Thermal Comfort in Buildings in Tropical Climate, Energy Procedia. 52 (2014) 250–259. https://doi.org/10.1016/j.egypro.2014.07.076.
[34] L. Koufi, Z. Younsi, Y. Cherif, H. Naji, Numerical investigation of turbulent mixed convection in an open cavity: Effect of inlet and outlet openings, Int. J. Therm. Sci. 116 (2017) 103–117. https://doi.org/10.1016/j.ijthermalsci.2017.02.007.
[35] Y. Khattari, M. Benghoulam, A. Arid, T. Elrhafiki, Numerical Study of a Ventilated Room: Effect of Heating Floor and Cooling Ceiling, in: 2017 Int. Renew. Sustain. Energy Conf. IRSEC, 2017: pp. 1–6. https://doi.org/10.1109/IRSEC.2017.8477344.
[36] D. Blay, S. Mergui, C. Niculae, Confined turbulent mixed convection in the presence of horizontal buoyant wall jet, Fundam. Mix. Convect. Heat Transf. Div. 213 (1992) 65–72.
[37] K. Zhang, D. Zhao, X. Yin, R. Yang, G. Tan, Energy saving and economic analysis of a new hybrid radiative cooling system for single-family houses in the USA, Appl. Energy. 224 (2018) 371–381. https://doi.org/10.1016/j.apenergy.2018.04.115.
[38] C. Teodosiu, V. Ilie, R. Teodosiu, Numerical Prediction of Thermal Comfort and Condensation Risk in a Ventilated Office, Equipped with a Cooling Ceiling, Energy Procedia. 85 (2016) 550–558. https://doi.org/10.1016/j.egypro.2015.12.243.
[39] L.F. Cabeza, A. Castell, C. Barreneche, A. de Gracia, A.I. Fernández, Materials used as PCM in thermal energy storage in buildings: A review, Renew. Sustain. Energy Rev. 15 (2011) 1675–1695. https://doi.org/10.1016/j.rser.2010.11.018.
[40] L'Agence Marocaine de l'Efficacité Energétique (AMEE), Règlement Thermique de Bâtiment au Maroc, 2015.
[41] G. Zhou, Y. Yang, H. Xu, Performance of shape-stabilized phase change material wallboard with periodical outside heat flux waves, Appl. Energy. 88 (2011) 2113–2121. https://doi.org/10.1016/j.apenergy.2011.01.016.